J Supercond Nov Magn (2011) 24: 675–678
DOI 10.1007/s10948-010-0932-4

ORIGINAL PAPER

Properties of Iron Oxide Nanoparticles Synthesized at Different Temperatures

Oznur Karaagac · Hakan Kockar · Taner Tanrisever

Received: 13 September 2010 / Accepted: 14 September 2010 / Published online: 16 October 2010

Abstract Iron oxide nanoparticles were synthesized by co-precipitation in air atmosphere at different temperatures and their structural and magnetic properties were investigated. The mean particle sizes of iron oxide nanoparticles were calculated from the X-ray diffraction (XRD) patterns using the Scherrer equation. Fourier transform infrared spectroscopy analysis exhibited the vibration bands at 563 cm^{-1} and 620 cm^{-1} confirming the formation of Fe_3O_4 and γ-Fe_2O_3, respectively. Morphological observation was made by a transmission electron microscope and the particle size of iron oxide nanoparticles was found to be around 9 nm which is consistent with the particle size calculated according to the XRD patterns. It was observed that the intensity of the peaks in the patterns and crystallinity increased as the temperature increased. Magnetization curves showed zero coercivities indicating that the samples are superparamagnetic.

Keywords Co-precipitation · Iron oxide nanoparticles · Superparamagnetic

O. Karaagac (✉) · H. Kockar
Physics Department, Science & Literature Faculty,
Balikesir University, 10145 Cagis, Balikesir, Turkey
e-mail: karaagac@balikesir.edu.tr

O. Karaagac (✉)
e-mail: oznurk00@hotmail.com

T. Tanrisever
Chemistry Department, Science & Literature Faculty,
Balikesir University, 10145 Cagis, Balikesir, Turkey

1 Introduction

Superparamagnetic iron oxide nanoparticles are very attractive for a broad range of biomedical applications having said that their magnetization is nearly zero without external magnetic field and the risk of forming agglomerates is negligible at room temperature [1]. A number of suitable techniques have been developed to synthesize magnetic nanoparticles. Sol–gel synthesis [2], hydrothermal reactions [3], microemulsions [4], co-precipitation [5] can be used for the synthesis of iron oxide nanoparticles. However, co-precipitation is most probably the simplest and most common method for the production of iron oxide nanoparticles obtained from iron salts, and has also the advantage of synthesizing large amount of nanoparticles. It is known that the structural properties of nanoparticles can be substantially influenced by the synthesis conditions such as temperature [6]. In this study, synthesis of iron oxide nanoparticles was performed by co-precipitation at different temperatures and the structural and magnetic properties of these nanoparticles were investigated and presented.

2 Experimental

Ferrous chloride tetrahydrate ($FeCl_2 . 4H_2O$ Merck >99%) and ferric chloride hexahydrate ($FeCl_3 . 6H_2O$ Merck >99%) salts and ammonium hydroxide (NH_4OH Merck, 25% of ammonia) were used for the synthesis of iron oxide nanoparticles. All chemicals were of reagent grade and used without further purification. $FeCl_2$ and $FeCl_3$ were dissolved in 50 ml deionized water with molar ratio of 2/3. 30 ml of ammonium hydroxide (25%) was diluted to 50 ml and added to 50 ml mixture of iron salts under a vigorous mechanical stirring. The reaction period was 30 minutes and each one was

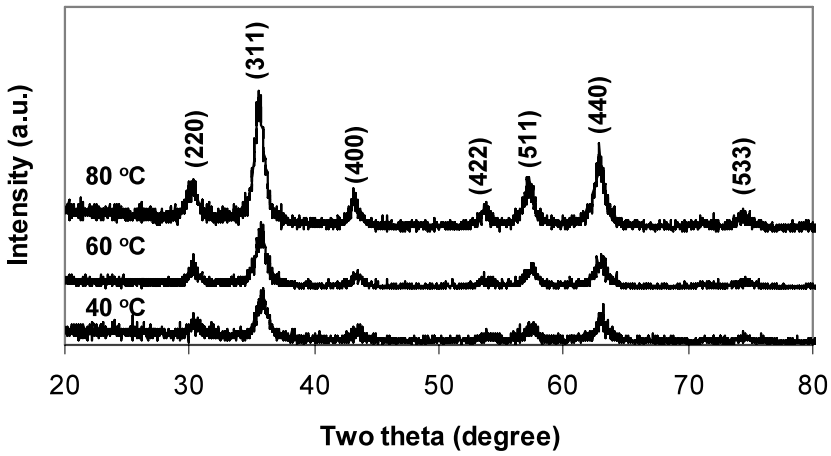

Fig. 1 XRD patterns of iron oxide nanoparticles synthesized at different temperatures

performed at the temperatures of 20, 40, 60, and 80 °C in air medium. After the reaction, the precipitate was washed three times with distilled water. To obtain the powder, the precipitate was dried in an oven.

The crystalline structure of nanoparticles was investigated with Rigaku-rint 2200 X-ray diffractometer system (XRD) using CuK_α radiation ($\lambda = 1.54056$ Å) between 20° and 80°. The samples were characterized by Fourier transform infrared spectroscopy (FTIR, Perkin Elmer-1600 Series). High resolution transmission electron microscope (HRTEM, FEI TECNAI G2 F30 model) with an accelerating voltage of 200 kV was used to obtain information about the size and also morphology of the nanoparticles. The particle sizes were obtained from TEM images by using the software ImageJ. The magnetic properties of nanoparticles were studied by vibrating sample magnetometer (VSM, ADE Technologies EV9) at ±20 kOe.

3 Results and discussion

Figure 1 shows X-ray patterns of the samples synthesized at different temperatures. The patterns show characteristic (220), (311), (400), (422), (511), (440), and (533) peaks of iron oxide at around $2\theta \approx 30°$, 35°, 43°, 53°, 57°, 63°, and 74°, respectively. All samples show a cubic spinel structure according to the JCPDS 019-0629 and JCPDS 039-1346 cards. It was observed in the patterns that the peaks intensified with the increase of temperature indicating that the crystallinity becomes stronger; see Fig. 1. The mean particle sizes, D_{XRD} of iron oxide nanoparticles synthesized at 20, 40, 60, and 80 °C calculated from the most intense peak (311) using the Scherrer equation were 8.88, 8.19, 8.18, and 9.48 nm, respectively. Liu et al. [7] reported that decreasing the preparation temperature results in a remarkable broadening of the peaks, which is due to the size effect and the particle size increases with the increase of temperature.

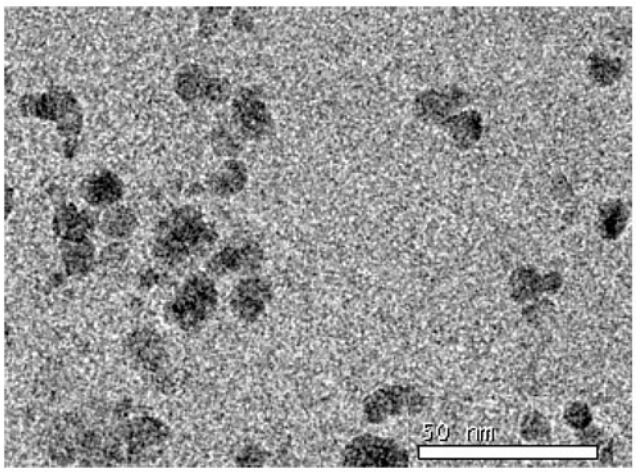

Fig. 2 TEM image of iron oxide nanoparticles synthesized at 20 °C (*scale bar*: 50 nm)

However, Babes et al. [8] said that the synthesis temperature (20–50 °C) showed little or no influence in their experimental setup. The results in this study showed that the particle sizes were nearly unaffected by the difference of the preparation temperature that is compatible with the study of Babes et al. [8]. The particle size of iron oxide nanoparticles synthesized at 20 °C is found to be 8.66 ± 3.74 nm and corresponding TEM image is demonstrated in Fig. 2. The size obtained from the TEM image matched with the size obtained from the XRD pattern. It was observed that iron oxide nanoparticles are not agglomerated.

FT-IR analysis was performed to affirm the structure of the product and the spectra of the samples are shown in the 1400–400 cm^{-1} region in Fig. 3. The transmittance peak of the sample synthesized at 20 °C which is at 563 cm^{-1} confirms the Fe_3O_4 formation and the peak observed at around 620 cm^{-1} declares the γ-Fe_2O_3 [9]. Other samples also show the same peaks of the similar spectrums.

Magnetization curves of the nanoparticles measured at ±20 kOe and the detailed curves drawn at ±30 Oe are

shown in Fig. 4. It is revealed that the magnetization curves at each temperature show no hysteresis that both the remanance and coercivity are zero. The results indicate that the iron oxide nanoparticles are single domain and show superparamagnetic nature at room temperature as it is expected for the nanoscale dimension of the particles [10]. The saturation field, H_s decreases from 11833 Oe to 10433 Oe with the increase of temperature. Saturation magnetization, M_s of the samples is between 65.40 and 67.72 emu/g that is lower than the bulk M_s value of magnetite (90–92 emu/g) but near to maghemite (∼80 emu/g) [11]. Therefore, a considerable ratio of maghemite phase accompanying the magnetite phase should also be taken into consideration as indicated by the FTIR spectrum. It is also observed that the slight change in the particle sizes might result in the slight change of the M_s. The mean magnetic particle size, D_{MAG} and standard deviation, σ can be calculated according to Chantrell et al. [12], who assume a log-normal size distribution [13]. The D_{MAG} and σ were calculated as 7.01 ± 0.55, 7.16 ± 0.49, 7.22 ± 0.52, and 7.14 ± 0.49 nm for iron oxide nanoparticles synthesized at 20, 40, 60, and 80 °C, respectively. D_{MAG} which is calculated as about 7 nm is smaller than that observed from TEM image, D_{TEM}. A number of possible mechanisms could explain the demagnetization of the particles but the simplest one was to assume that the surface layer of iron oxide atoms does not contribute to the magnetic properties of the particles [7]. Thus, the magnetically dead layer [14] on the particle surface explains the difference between D_{MAG} and D_{TEM}.

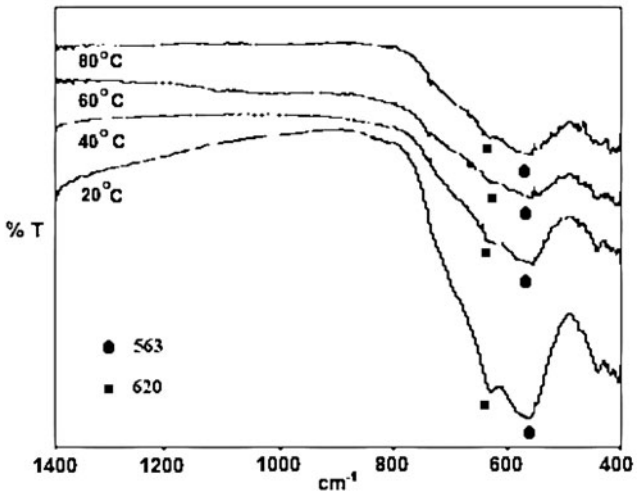

Fig. 3 FT-IR spectrum of iron oxide nanoparticles precipitated at different temperatures

4 Conclusions

The structural analysis of the synthesized nanoparticles showed the iron oxide structure and FTIR analysis showed the peaks of Fe_3O_4 and γ-Fe_2O_3. It is seen that the crystallinity increased with the increase of reaction temperature. Physical particle sizes calculated from XRD patterns and obtained from TEM images are consistent with each other and around 9 nm. The remenant magnetization and coercivity are found to be zero indicating the superparamagnetic nature of the iron oxide nanoparticles, and the magnetic sizes of all samples calculated from the hysteresis curves were found to be almost the same that were around 7 nm.

Acknowledgement This work was supported by Balikesir University Research Grant no. BAP 2010/35. The authors would like to thank the State Planning Organization, Turkey, under Grant no 2005K120170 for VSM system. O. Karaagac would like to thank TUBITAK for the BIDEB 2211 Scholarship. The authors also thank Department of

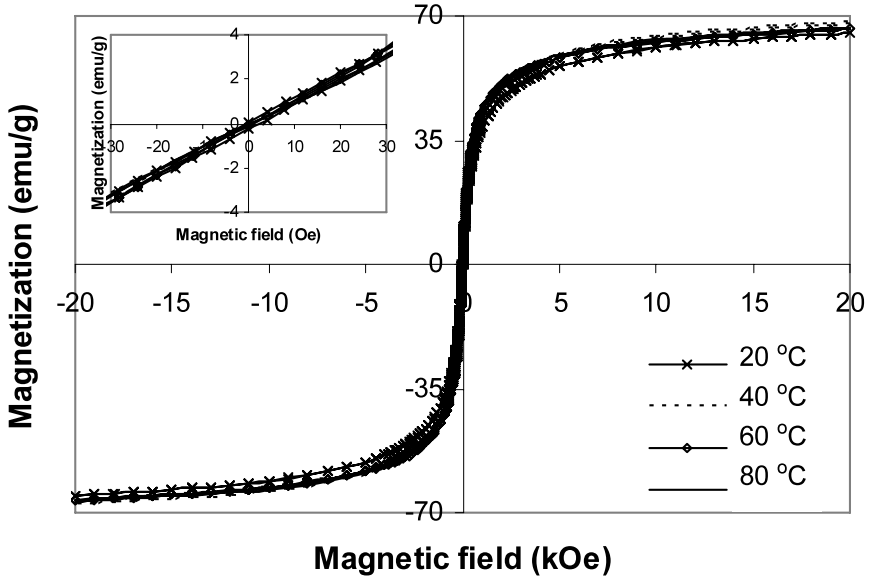

Fig. 4 Magnetization curves of iron oxide nanoparticles. *Inset* shows the enlarged views at ±30 Oe

Materials Science and Engineering, Anadolu University, Turkey for XRD measurements, the Chemistry Department, Balikesir University, Turkey for FT-IR measurements, and the National Nanotechnology Research Center (UNAM), Bilkent University for TEM analysis.

References

1. Lu, A.H., Salabas, E.L., Schüth, F.: Angew. Chem. Int. Ed. **46**, 1222 (2007)
2. Zhou, S.M., Zhao, S.Y., He, L.F., Guo, Y.Q., Shi, L.: Mater. Chem. Phys. **120**, 75 (2010)
3. Fan, R., Chen, X.H., Gui, Z., Liu, L., Chen, Z.Y.: Mater. Res. Bull. **36**, 497 (2001)
4. Aubert, T., Grasset, F., Mornet, S., Duguet, E., Cador, O., Cordier, S., Molard, Y., Demange, V., Mortier, M., Haneda, H.: J. Colloid Interface Sci. **341**, 201 (2010)
5. Kim, D.K., Mikhaylova, M., Zhang, Y., Muhammed, M.: Chem. Mater. **15**, 1617 (2003)
6. Gnanaprakash, G., Mahadevan, S., Jayakumar, T., Kalyanasundaram, P., Philip, J., Raj, B.: Mater. Chem. Phys. **103**, 168 (2007)
7. Liu, Z.L., Liu, Y.J., Yao, K.L., Ding, Z.H., Tao, J., Wang, X.: J. Mater. Synth. Process. **10**(2), 83 (2002)
8. Babes, L., Denizot, B., Tanguy, G., Le Jeune, J.J., Jallet, P.: J. Colloid Interface Sci. **212**, 474 (1999)
9. Namduri, H., Nasrazadani, S.: Corros. Sci. **50**, 2493 (2008)
10. Jain, N., Wang, Y., Jones, S.K., Hawkett, B.S., Warr, G.G.: Langmuir **26**(6), 4465 (2010)
11. Hunt, C.P., Morkowitz, M.B., Banerjee, S.K.: Rock physics and phase relations. In: A Handbook of Physical Constants, p. 196. American Geophysical Union, Washington (1995)
12. Chantrell, R.W., Popplewell, J., Charles, S.W.: Physica B+C **86–88**, 1421 (1977)
13. O'Grady, K., Bradbury, A.: J. Magn. Magn. Mater **39**, 91 (1983)
14. Kaiser, R., Miskolczy, G.: J. Appl. Phys. **41**, 1064 (1970)